Polar Science 20 (2019) 129–135

Contents lists available at ScienceDirect

Polar Science

journal homepage: www.elsevier.com/locate/polar

Geometric changes of three glaciers in Dickson Land, central Spitsbergen, during the period 1990–2015

Barbora Procházková*, Zbyněk Engel, Jiří Tomíček

Charles University, Faculty of Science, Department of Physical Geography and Geoecology, 128 43, Prague, Czech Republic

ARTICLE INFO

Keywords:
Ground penetrating radar
Digital elevation model
Ice thickness
Glacier volume
Central Spitsbergen

ABSTRACT

Glaciers of the Svalbard archipelago react very rapidly to climate change in the polar environment. Combining the study of aerial photographs, digital elevation models and in situ measurements, it is possible to measure glacier geometric changes. Apart from the standard remote sensing data evaluation we focus on in situ measurements by ground penetrating radar. This study calculates length, area, volume and elevation changes of three glaciers in Dickson Land, central Spitsbergen, during the period 1990–2015. Ground penetrating radar surveys indicate ice thickness, which was used for calculating the volume and the bed topography of the glaciers. The mean ice thickness ranges from 21.2 to 52.4 m. Between 1990 and 2015, the glacierized area decreased from 5.37 ± 1.02 km^2 to 4.45 ± 0.25 km^2 (- 17.5%) and the volume reduced from 309.93 ± 4.75 mil m^3 to 215. 44 ± 1.27 mil m^3 (- 30.5%). The mean surface elevation decreased by 23.0 ± 8.4 m (Bertilbreen), 22.3 ± 10.2 (Ferdinandbreen) and 10.7 ± 7.8 m (Elsabreen). The average surface elevation (0.4 ± 0.3 to 1.0 ± 0.4 m a^{-1}) and volumetric (- 0.22 ± 0.02 to - 3.61 ± 0.12 mil m^3 a^{-1}) changes correspond to values reported from this and other regions of Svalbard.

1. Introduction

Glaciers and ice caps in the Arctic region are one of the major glacier repositories in the World. These ice masses are among the largest contributors to sea-level rise and caused about 30% of the measured sea-level rise between 2004 and 2010 (SWIPA, 2017). However, melting of relatively small mountain glaciers contributes to sea-level rise of the same magnitude as that of the largest ice sheets (IPCC, 2013) and it is expected to dominate sea level rise in 21st century (Radić et al., 2014; Slangen et al., 2014). Therefore, it is of great importance to know the volume of these glaciers which have a relatively short response time to climate change (Bach et al., 2018 and references therein). While areal changes of small glaciers could be relatively easily detected with remote sensing methods, ice thickness and glacier volume is possible to infer only on the base of scaling methods or from field surveys. The ground penetrating radar (GPR) survey is the most frequently used tool for obtaining information about the ice thickness and volume of these glaciers.

Glaciers in Svalbard cover approximately 60% of its area (34 600 km^2) with a total volume of 7000 km^3 (Moholdt et al., 2010; Hagen et al., 2003). Despite the large extent of the glaciated area, only few ice thickness and volume data are available for glaciers in this region. Most of regional studies have determined glacier volume based on topographic elevation data (König et al., 2014), which have limited vertical resolution. Ice volume calculated based on in-situ measurements are known only for fraction of glaciers on Svalbard (e.g. Martin-Español et al., 2015). The sequences of aerial photographs (NPI, 1990, 2009) and position of frontal moraines indicate that most Svalbard glaciers have been retreating since the culmination at the LIA in the end of 19th century. During the LIA, the area covered by glaciers was 38 871 km^2, and since then, the glaciers decreased by 5096 km^2 (-13.1%) (Martín-Moreno et al., 2017). This recession and thinning of glaciers is the most prominent in the central part of Spitsbergen – Dickson Land. In Dickson Land, the area covered by glaciers has decreased by 38% since the end of the LIA and thinning of glaciers is significant also in higher elevations up to 1000 m a.s.l. (Malecki, 2016). In contrast, recent data of satellite altimetry shows balance or thickening in high-elevation of major ice masses in north-eastern Svalbard (Moholdt et al., 2010; Nuth et al., 2010).

The Arctic area has experienced more warming over the last 2 -3 decades that any other region on the World (Førland et al., 2011). The mean annual temperature in Svalbard has increased by 2.5 °C when comparing the periods 1961–1990 and 1991–2017 (Norwegian Meteorological Institute, 2019a), the trend in rising annual temperature is about 0.7 °C per decade (James et al., 2012). The volume loss of glaciers reflects the rising temperatures and climate change of this

* Corresponding author.
E-mail address: prochazb@natur.cuni.cz (B. Procházková).

https://doi.org/10.1016/j.polar.2019.05.004
Received 25 August 2018; Received in revised form 6 May 2019; Accepted 8 May 2019
Available online 10 May 2019
1873-9652/

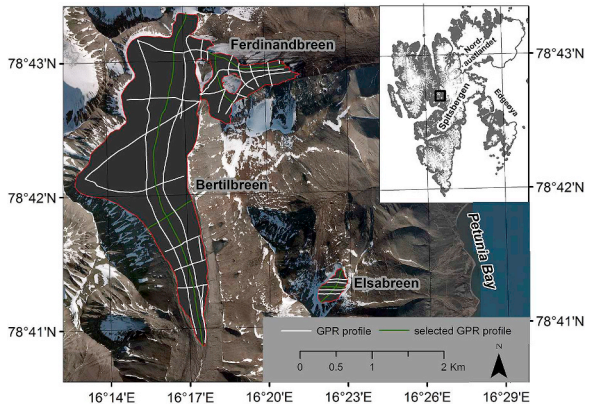

Fig. 1. Location of the studied glaciers and layout the GPR profiles (white lines). Selected GPR profiles in green are shown on Fig. 3 and 4.

region (Moholdt et al., 2010; Nuth et al., 2010; Kohler et al., 2007, Malecki 2013a).

The primary objective of this study is to estimate ice thickness and volume for three glaciers with different size in the central part of Svalbard. We also present the length, areal, elevation and volumetric changes of these glaciers. The changes of the length, surface area and elevation between 1990 and 2015 were derived from comparing aerial photographs and digital elevation models (DEMs), respectively. Apart from the standard remote sensing data evaluation we focus on in situ measurements by Ground penetrating radar (GPR). Ground penetrating radar surveys indicate ice thickness, which was used for calculating the volume and the bed topography of the glaciers. We emphasize the comparison between elevation changes in our and other studies from Svalbard, which show a similar trend in elevation changes in the recent years.

Three land-terminating glaciers in the central Spitsbergen (Dickson Land) were investigated in this study. Bertilbreen (BB) and Ferdinandbreen (FB) are small valley glaciers, while the smallest Elsabreen (EB) represents a niche glacier (Fig. 1; Table 1). The investigated glaciers are located approximately 50 km to the north of the weather station at the Svalbard Airport (15 m a.s.l.). The mean annual air temperature (1991–2017) of - 4.0 °C was recorded at this weather station, with the summer mean (JJA) of 5.4 °C and winter mean (DJF) of - 10.7 °C (Norwegian Meteorological Institute, 2019a-b). Between 1991 and 2017 the mean annual precipitation was 199 mm yr^{-1} (Norwegian Meteorological Institute, 2019c). Mean monthly precipitation is at a minimum during the spring period (31 mm, MAM), while the maximum is measured in the autumn period (58 mm, SOM) at most of the weather stations in Svalbard (Førland et al., 2011).

Dickson Land occupies 200 km^2, of which only about 14% is covered by glaciers (Malecki, 2013a). This area is relatively arid and as a result of this, glaciers there are small and mostly restricted to valleys and cirques. Glaciers of this region are mostly cold or polythermal with cold ice and temperate layer of surface ice in summer or temperate ice beneath the thickest part of the glacier (Malecki, 2013b). Volume characteristics are known only for a minority of them (Malecki, 2016; Martin-Español et al., 2015). Apart from this region, ice thickness data provided by GPR surveys were collected on Ariebreen in Hornsund (Laparazan et al., 2013), Pedersenbreen in north-western Spitsbergen (Ai et al., 2014), Hornbreen-Hambergbreen glacier system in southern Spitsbergen (Palli et al., 2003) and on eight glaciers in Wedel Jarlsberg Land (Navarro et al., 2014).

2. Material and methods

2.1. Field survey

In the summer periods of 2013–2015, three field campaigns were carried out to determine glacier extent, surface elevation and ice thickness. The GPR and differential GPS (dGPS) survey was carried out in summer 2013 (BB) and 2015 (FB and EB). The dGPS measurements were realized using Trimble GeoExplorer S6000 receiver (TRIMBLE, 2009). Firstly, the base station was placed on the western shore of Petunia Bay. The distance between the base station and sites of measurement was up to 6 km. The dGPS data were collected to determine the glacier extent and surface elevation and to obtain ground control points for reference aerial photographs. The ground control points were selected as stable features in terrain (e.g. rock-outcrop). The surface elevation was measured approx. in 100-m-step intervals, each measurement lasted 2 min. The measured dGPS data were corrected using Trimble Pathfinder Office software (TRIMBLE, 2008). For the interpolation of surface elevation, only points with vertical accuracy up to 0.5 m were used. The dataset of surface elevation contains 302 points in total for BB, 45 points for FB and 79 points for EB.

The GPR survey (Fig. 1) was carried out with an unshielded 50 MHz Rough Terrain Antenna and a RAMAC CU-II control unit (MALÅ Geoscience, 2005). The signal acquisition time was set to 906–1124 ns, scan spacing was 0.1 m and the distance between antennas (T_x – R_x) was 4.2 m. The Garmin GPSMAP 60CSx receiver was used to determine the position of the GPR profiles. The GPR data were collected along 3 longitudinal and 12 transverse profiles on BB with the total length of 22 317 m. On FB and EB, the GPR measurements were carried out along 5 longitudinal and 7 transverse, profiles with the total length of 7840 m and 1 longitudinal and 5 transverse profiles with the length of 2300 m, respectively.

2.2. Aerial photographs and DEMs

The Norwegian Polar Institute (NPI) aerial photographs taken in 1990 and 2009 were used to extract information about length and extent of investigated glaciers. Images were registered using ground-control points (GCPs) and dGPS coordinates measured in the deglaciated landscape in the summer periods of 2013, 2014 and 2015. The 1990, 2009 photographs have a ground resolution of 1.2 m and 0.6 m, respectively. The root-mean-square error (RMSE) of registration of the images ranged from 4.2 to 19.2 m (Table 2) and was used as a horizontal accuracy.

The DEMs derived by the NPI from the 1990 aerial photographs were used to estimate surface elevation of the glaciers. The 1990 dataset has a ground resolution of 20 m and a horizontal and vertical uncertainty of less than 5 m (König et al., 2014). Ice elevation changes and mean lowering rates over the glaciers after 1990 were calculated using the aerial photographs-based DEMs and surface elevation models derived from the dGPS data collected during the field campaigns 2013

Table 1
Glaciological parameters of the investigated glaciers. The theoretical stready-state ELA was calculated by Malecki (2016) and the values are from 2009.

Glacier	Length (m)	Area (Km2)	Mean ice thickness (m)	Maximum Ice thickness (m)	Volume (mil m3)	Elevation range (m a.s.l.)	Theoretical stready-state ELA (m)
Bertilbreen (2013)	4871.7 ± 8.5	3.78 ± 0.06	52.5 ± 1.8	127.1 ± 4.8	206.56 ± 0.49	240–640	447
Ferdinandbreen (2014)	1289.8 ± 8.5	0.56 ± 0.03	13.3 ± 0.5	42.5 ± 1.5	6.81 ± 0.22	260–525	384
Elsabreen (2015)	553.1 ± 5.7	0.11 ± 0.02	21.2 ± 0.8	50.5 ± 1.8	2.07 ± 0.08	440–720	540

Table 2
Characteristics of the remote sensing data and the root-mean-square error of the registration.

	Pixel size at ground (m)	RMSE (m)
NPI Image 1990	1.2	19.2 (BB) 18.2 (FB) 4.2 (EB)
NPI Image 2009	0.6	8.5
Sentinel-2 Image	–	–
	–	–
	10	5.7 (EB)

and 2015 (see the next section for details).

2.3. Data processing and determination of glaciological parameters

The glaciers length was determined along central flowline of the investigated glacier. Estimated errors of the glacier length were determined as the RMSE of the georegistration of aerial photographs in a given year (horizontal accuracy). The length change error (ε_{dL}) was determined using the following formula (Hall et al., 2003):

$$\varepsilon_{dL} = \sqrt{\varepsilon_{Lx}^2 + \varepsilon_{Ly}^2}. \quad 1$$

ε_{Lx}^2 = the length error in 1990, ε_{Ly}^2 = the length error in the year of the GPR survey (2013–2015).

The 1990 glacier extent was derived from aerial photographs (NPI, 1990). The extent of the glacier in the GPR survey period was determined from GPS measurements with a mean horizontal accuracy of 5.4 m for BB and 6.12 m for FB for the year of the GPR survey. The extent of EB was derived from the Sentinel-2 image. The resolution and registration uncertainty (RMSE) were summed quadratically to estimate the total error. The area error was obtained by multiplying this total error by the perimeter of each glacier (Rivera et al., 2007).

The area change error was calculated in the same way as the length change error. Ice-divide between BB and FB was determined on the base of the GPR and passed over the area with ice thickness between 1 and 10.5 m (Fig. 2). Ice-divide between BB and Svenbreen in the uppermost part of BB was determined according to contour lines.

The GPR data were processed and interpreted using the REFLEXW software, version 4.5. (Sandmeier, 2008). The dewow filter was used to suppress low-frequency energy emitted by the field near the transmitter. The exponential gain function increased the strength of the signal with depth. Finally, the strong direct wave signal and noise reflection were eliminated using background removal. According to Baelum and Benn (2011) we applied a radio-wave velocity of 168 m μs^{-1} to convert two-way travel times to ice thickness values. The uncertainty of ice thickness determined from the GPR measurement was estimated using the following formula (Lapazaran et al., 2016):

$$\varepsilon_H = \frac{1}{2}\sqrt{\tau^2\varepsilon_c^2 + c^2\varepsilon_\tau^2} \quad 2$$

where τ is the normal moveout-corrected two-way travel time, εc is the uncertainty in radio-wave velocity, c is the radio-wave velocity in the medium and ετ is the timing error. We considered a conservative estimate of vertical resolution (a half of the signal's wavelength in glacier ice, i.e. 1.68 m for the 50 MHz antenna) and a relative error in radio-wave velocity of 3.6%, which corresponds to a range of velocity values from 165 to 171 m μs–1. We chose this narrow range since we anticipated only minor variations in ice and snow characteristics on the investigated glaciers. The snow cover thickness ranged from 0.1 to 0.4 m during the GPR survey and the snow was wet. Considering the densities between 350 and 450 kg m^{-3}, the error in the value of ice thickness due to snow ranged from 0.3 to 1.1%.

The 1990 surface elevation model was interpolated from contour lines with a 20 m interval. The glacier bed topography and surface elevation models for 2013 and 2015 were derived from the ice thickness and dGPS data, respectively. For the interpolation of the base elevation and surface elevation models we investigated three interpolation and geostatistical methods (inverse distance weighting, radial basis function and kriging) with various settings. Accuracy of the interpolation method was determined as the root-mean-square error (RMSE) based on cross-validation. Accuracy of the interpolation method was determined as the root-mean-square error (RMSE) based on cross-validation. The method examines the ability of the algorithm to interpolate the original data (Houlding, 2000). The data points are successively omitted and replaced by the interpolated value from the other data points. The difference between the actual and interpolated values is called an error (mean error or root-mean-square error). Both, the surface elevation model and the base elevation model were produced using the kriging geostatistical method, which had the lowest RMSE (Table 3). The grid cell size of the interpolated surface and base elevation model is 5.5 m. The RMSE of the interpolated elevation model are in range between 1.4 and 9.8 m.

The grid of the ice thickness was calculated as a difference between

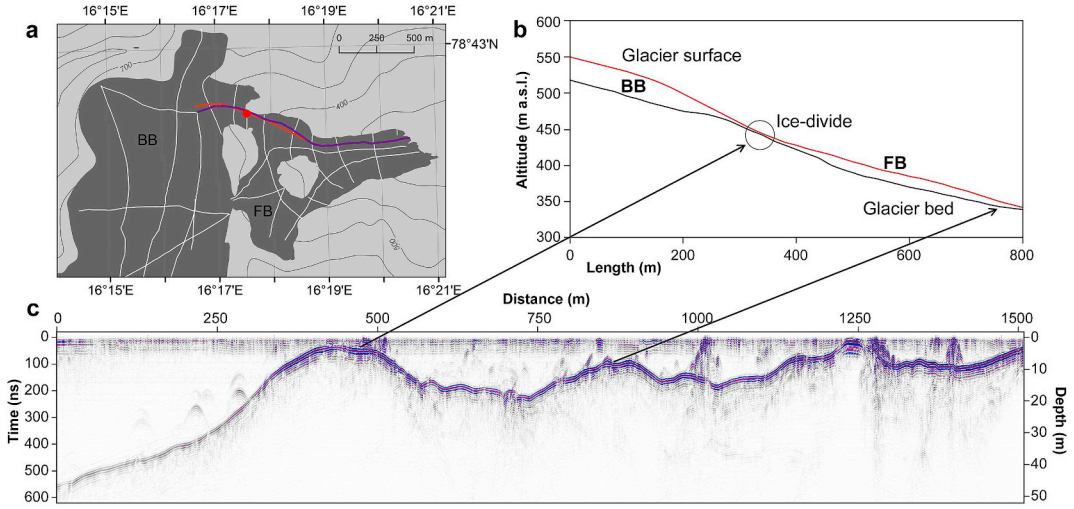

Fig. 2. Ice-divide between BB and FB based on the GPR survey. Red dot represents the ice-divide (a). Black and red lines represent the base and surface elevation, respectively (b). Ice-divide on GPR profile FB_010 (c). (For interpretation of the references to colour in this figure legend, the reader is referred to the Web version of this article.)

Table 3
RMSE of the interpolation of constructed DEMs.

	RMSE (m)					
	Bertilbreen		Ferdinandbreen		Elsabreen	
	1990	2013	1990	2014	1990	2015
Surface Elevation Model	5.0	1.4	5.0	4.7	5.0	1.9
Base Elevation Model	9.7	9.3	7.9	7.9	7.7	7.3

surface elevation and base elevation model. The surface elevation change was calculated as a difference between the glacier surface DEMs model derived from dGPS data and the digital elevation model from 1990. As the glacier extent was different in those years, the basal elevation model for 1990 needed to be supplemented by glacier limits in the period of the GPR measurement. The points from the GPR measurement and some extra points were used for a construction of the base elevation model in 1990. Some extra points in the ice-free area in the period of the GPR measurement were obtained from DEM 2009 (Norwegian Polar Institute, 2014). The overall vertical accuracy of the surface elevation change was determined as a sum of vertical accuracies of 1990 DEMs and recent surface elevation model.

The glacier volume was calculated as a difference between surface and base elevation models of the glaciers. The glacier volume error was estimated as a combination of ice thickness and area error. The volume change was calculated as a difference between the glacier volume in 1990 and the most recent one. Errors in glacier volume change were computed in the same way as error change of different glaciological parameters (Equation (1)).

3. Results

The GPR data indicate that all the investigated glaciers are predominately cold (Figs. 3 and 4). Concerning the fact that the ice of EB and FB is relatively thin, it is not surprising. Thin basal layer of temperate ice may exist under the thickest part of BB. Unfortunately, we were not able to observe scattering of temperate ice in GPR profiles done with 50 MHz antenna.

The GPR data reveal the ice thickness of the investigated glaciers (Fig. 5). Presence of water at the glacier surface may have caused some scattering in the upper part of the GPR profile, but in general, basal reflections were easily observed in all profiles (Figs. 3 and 4). The mean ice thickness of BB is 52.5 ± 1.9 m. At BB, the maximum ice thickness of 135.5 ± 4.8 m was measured in the lower part of its accumulation zone. The mean ice thickness of FB is lower than that of EB: 13.3 ± 0.5 m compared to 21.2 ± 0.8 m. The maximum thickness of FB is 42.1 ± 1.5 m. At EB, the greatest ice thickness was measured in the central part of the glacier, where the glacier is as much as 50.5 ± 1.8 m thick.

A decrease of surface elevation of BB reaches the mean value of

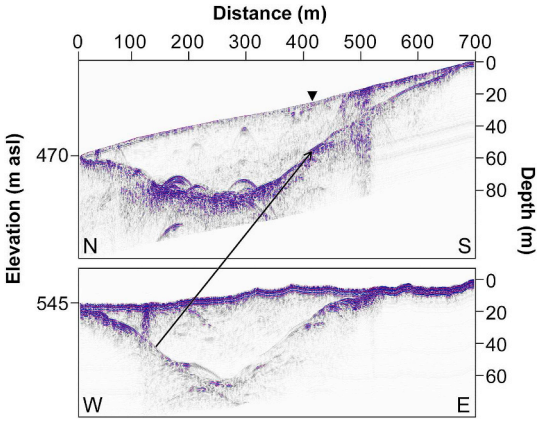

Fig. 4. Longitudinal (a) and cross-sectional (b) GPR transects for EB.

23.0 ± 8.4 m (Table 4; Fig. 6). During the investigated period, the length change of BB was - 220.0 ± 20.8 m (- 4.3%) and the area decreased by −0.30 ± 0.26 (−7.4%) (Fig. 7; Table 4). Surface elevation of FB decreased by 22.3 ± 10.2 m on average over the period 1990–2014 (Table 4). Between 1990and2014, FB lost 263.2 ± 19.0 m (- 16.9%) of its length and 0.26 ± 0.10 km^2 (31.4%) of its area (Fig. 7; Table 4). The surface elevation of EB decreased on average by 10.7 ± 7.8 m between 1990 and 2015 (- 0.4 ± 0.3 m a^{-1}). The largest areal and length changes were observed at EB (Fig. 7): the changes are - 834.9 ± 7.1 m (- 60.2%) and −0.34 ± 0.07 km^2 (−75.1%), respectively.

The volume of BB decreased from 289.56 ± 3.01 mil m^3 to 206.56 ± 0.49 mil m^3 between 1990 and 2013 (Table 4). EB and FB experienced volume loss of 5.38 ± 0.33 mil m^3 (- 74.2%) and 6.29 ± 0.87 (- 48.1%) mil m^3, respectively. The maximal volume change was calculated for the smallest glacier EB.

4. Discussion and interpretation

4.1. Length and areal changes between 1990 and 2015

Observed length and areal decreases correspond to the size of glaciers, so smaller glaciers (EB and FB) retreated and lost its area at a greater rate than the largest glacier BB. The greatest recession rate was observed at EB, which is confirmed by its annual recession rate of 44.9 ± 0.6 m.a^{-1} reported by Malecki (2016). EB, as the smallest glacier, responds to climate change most rapidly among the investigated glaciers. Values of annual areal recessions are between 0.012 ± 0.004 to 0.002 ± 0.001 km^2 a^{-1}. Rachlewicz et al. (2007) found that annual areal changes were between 0.002 and 0.053 km^2 a^{-1} (1960–1990) compared to 0.004–0.092 km^2 a^{-1} (1990–2002). Areal changes observed in the investigated glaciers in this study are within the values of the 90s reported by Rachlewicz et al. (2007). The

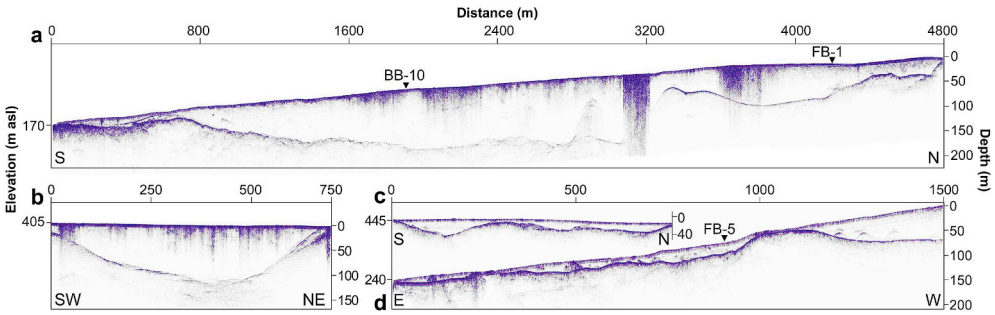

Fig. 3. Longitudinal and cross-sectional GPR transects for BB (a, b) and FB (c, d). Arrows and inverted triangles indicate glacier bed and points of crossover of the selected profiles, respectively.

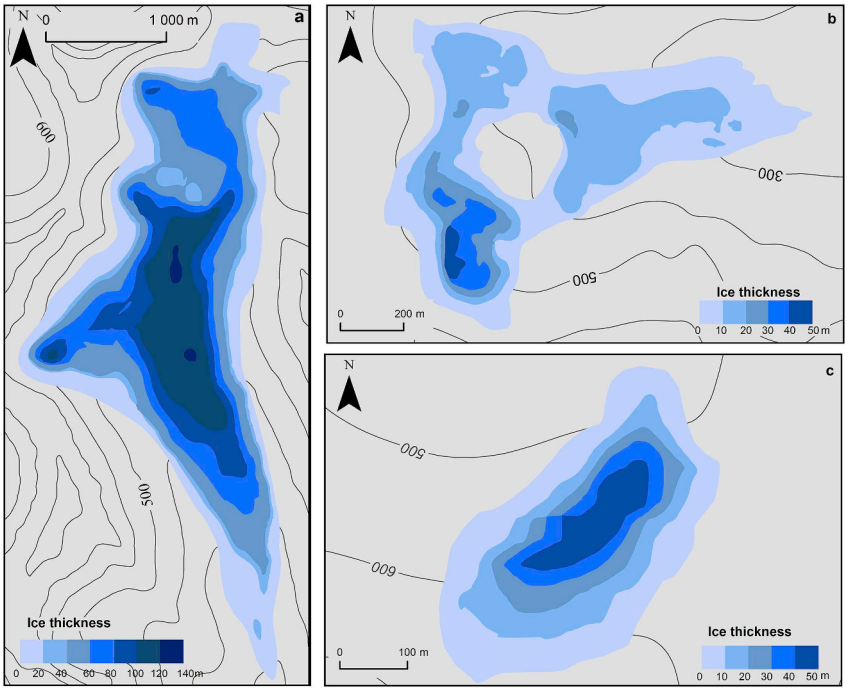

Fig. 5. Maps of the ice thickness of BB in 2013 (a), EB in 2015 (b) and FB in 2014 (c) determined from GPR survey. Contour line interval is 100 m.

Table 4
The changes of the glaciological parameters of the investigated glaciers between 1990 and 2015.

Glacier	Length (m)		Area (Km2)		Surface elevation change (m)	Annual change of the surface elevation (m.a)	Volume (mil m3)	
	change	annual	change	annual change			change	annual
Bertilbreen (1990–2013)	220.0 ± 20.8 (−4.3%)	9.7 ± 0.9	- 0.30 ± 0.26 (−7.4%)	0.012 ± 0.011	- 23.0 ± 8.4	- 1.017 ± 0.365	- 83.00 ± 3.11 (- 28.6%)	- 3.61 ± 0.12
Ferdinandbreen (1990–2014)	263.2 ± 19.0 (−16.9%)	11.0 ± 0.8	- 0.26 ± 0.10 (−31.4%)	0.012 ± 0.004	- 22.3 ± 10.2	- 0.930 ± 0.422	- 6.29 ± 0.71 (48.1%)	- 0.26 ± 0.03
Elsabreen (1990–2015)	834.9 ± 7.1 (−60.2%)	33.4 ± 0.3	- 0.34 ± 0.07 (−75.1%)	0.013 ± 0.002	- 10.7 ± 7.8	- 0.426 ± 0.311	- 5.38 ± 0.50 (74.2%)	- 0.22 ± 0.02

primary cause of the recession rate is an increase in mean temperatures: the mean temperature has increased by 2.5 °C comparing the period 1960–1990 and 1991–2017 (Norwegian Meteorological Institute, 2019a). Trends in seasonal mean temperatures at Svalbard Airport show a temperature increase for all four seasons: the largest increase in temperature per decade from 1899 to 2016 is in winter and spring: 0.3 °C and 0.4 °C, respectively (Norwegian Meteorological Institute, 2019b).

4.2. Surface elevation and volumetric changes

The mean surface lowering in the studied glaciers ranged from - 0.4 ± 0.3 to - 1.0 ± 0.4 m a^{-1} (with a mean value 0.8 ± 0.4 m a^{-1}) and thus reflected the regional pattern of changes reported by Malecki (2013a); 2016). Malecki (2013a) analysed the mean thinning of glaciers of seven glaciers in Dickson Land: in his study he documented the mean thinning of - 0.78 m a^{-1} (between 1990 and 2009), which is twice the value for the period 1960–1990 (i.e. - 0.49 m a^{-1}). The increased average rate of glacier thinning is reported from other parts of Svalbard too (Kohler et al., 2007). Our estimates of surface lowering are in agreement with studies from different parts of Svalbard. For instance Kohler et al. (2007) documented the mean surface lowering of 0.69 m a^{-1} for two small land-terminating glaciers in the western Svalbard over the period 2003–2005. A similar mean value of 0.76 ± 0.10 m a^{-1} is reported by James et al. (2012) for six glaciers all over the Svalbard after 1990.

The annual surface lowering was 1.0 ± 0.4 m a^{-1} (BB), 0.9 ± 0.4 m a^{-1} (FB) and 0.4 ± 0.3 m a^{-1} (EB). The lower surface elevation change at EB could be explained by high elevation of the glacier (440–720 m a.s.l.) and favourable north-eastern exposition. Malecki (2016) found theoretically steady-state ELA for EB in 540 m a.s.l., the major part of the glacier is still above this line. Values of this glacier thinning correspond well with the mean glacier thinning between 0.08 ± 0.26 to 1.06 ± 0.99 m.a^{-1} (with mean value of 0.71 ± 0.05 m.a^{-1}) calculated for Dickson Land by Malecki (2016) over the period 1990–2009. In the case of EB, however, we estimate half the value reported by Malecki (2016). This could be explained by different DEMs used for the calculation of surface elevation change. Malecki (2016) computed elevation change by subtracting the 1990 DEM from the 2009 DEM, which has a lower resolution than our 2015 DEM. However, the lower value of surface decrease at EB could also be explained by different time period. Rapid temperature rise in the 1990s decelerated between 2005 and 2010 (Førland et al., 2011). This could cause the shift of ELA to lower altitudes and thus the small gain of the ice of EB could lower the value of the mean surface decrease reported in our study.

At EB, a low surface elevation decrease was observed at elevation up to 710 m a.s.l. This is in line with earlier studies (Malecki, 2013a and 2016), where thinning of glaciers was observed up to 1000 m a.s.l. The thinning of glaciers at high elevation can be attributed to a rise in summer temperatures and albedo decrease in the upper parts of the glaciers, where snow and firn is disappearing and bare ice is revealed

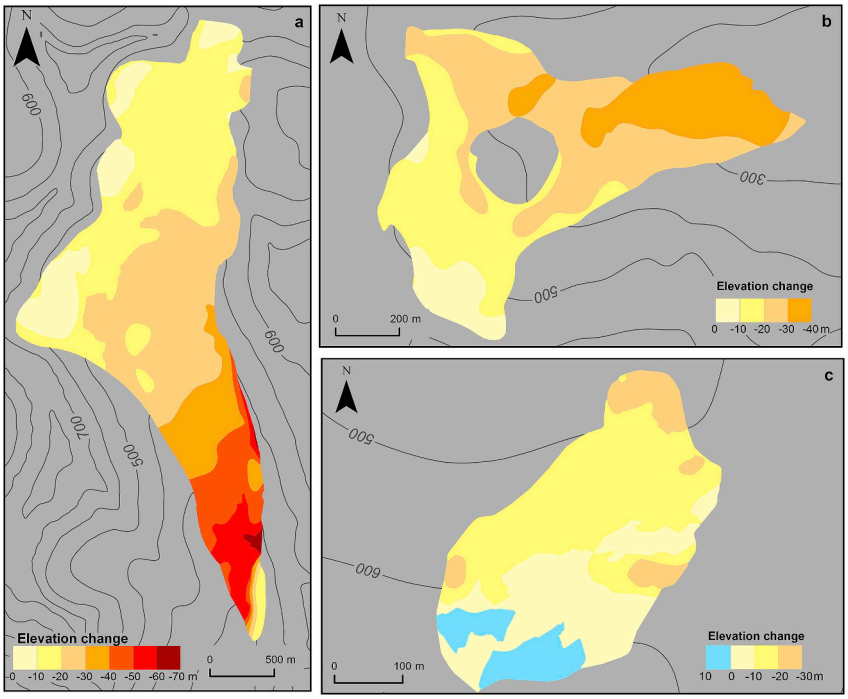

Fig. 6. Spatial distribution of the elevation changes of BB for the period 1990–2013 (a), EB between 1990 and 2015 (b) and FB between 1990 and 2014 (c). Contour line interval is 100 m.

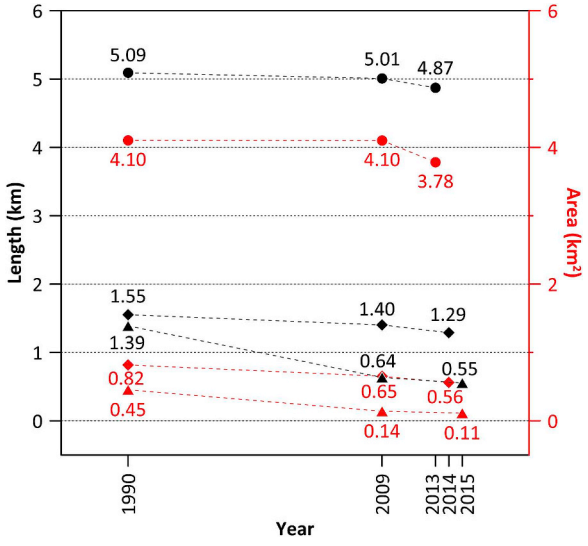

Fig. 7. The length (black colour) and areal (red colour) changes of the investigated glaciers between 1990 and 2015. BB is depicted as a dot, FB is depicted as a rhombus and EB as a triangle symbol. (For interpretation of the references to colour in this figure legend, the reader is referred to the Web version of this article.)

(Malecki, 2016). The mean summer (JJA) temperature increase is 0.51 °C a^{-1} over the period 1992–2012, compared to 0.28 °C a^{-1} for the period 1961–1991 (Norwegian Meteorological Institute, 2019b). The high rate of surface lowering will lead to a considerable or complete melt-out of all the investigated glaciers during 21st century if the atmospheric warming trends continue. In Svalbard, the predicted warming is between 3 and 8 °C by the end of the 21st century, according to climate projections of IPCC (IPCC, 2007).

The spatial distribution of decrease in ice thickness indicates that all the investigated glaciers have been evolving similarly: the surface elevation decrease maximum occurred in the lower part of the glaciers, while minimal changes or slight increases of surface elevation were observed in the upper part. BB and FB experienced a negative change on its whole area. FB has the smallest maximum and mean ice thickness among the investigated glaciers. Although the smallest glacier EB is thicker than FB, EB will be the first of the studied glaciers to disappear. Assuming a constant rate of volume loss, EB will disappear in the next 10 years.

Accelerating ice loss is observed from other parts of the Arctic. The glaciers of Frans Josef Land archipelago in the Russian Arctic are also subject to enhanced ice loss: mass loss doubled between 2011 and 2015 compared to the period 1953–2011 (Zheng et al., 2018). The intensive ice loss was found to be caused by increase in the regional temperature: mean air temperatures have increased at double the average global rate over the past few decades in the Arctic (Serreze and Francis, 2006).

The volume loss between 0.21 ± 0.02 mil m^3 a^{-1} and 3.61 ± 0.12 mil m^3 a^{-1} observed in the study area is well within the values range between 0.01 ± 0.08 mil m^3 a^{-1} to 6.78 ± 0.58 mil m^3 a^{-1} reported by Malecki (2016). In the case of BB, the volume loss was - 3.61 ± 0.12 mil m^3 a^{-1}, which is within the limits of - 3.23 ± 0.39 mil m^3 a^{-1} reported for the period 1990–2009 by Malecki (2016). The values of volume change on smaller glaciers EB and FB, are lower than the values reported by Malecki (2016). On FB, Malecki (2016) reported the annual volume loss 0.86 mil m^3 a^{-1} compared to our value 0.26 ± 0.03 mil m^3 a^{-1}. This difference could result from different delimitation of the glacier. In our case we calculated volume change only for the main glacier body. Malecki (2016) calculated volume change also for small ice fields which separated from the main glacier body between 1960 and 1990.

5. Conclusion

The largest of the investigated glaciers BB retreated by 220.0 ± 20.8 m between 1990 and 2013. The area of BB decreased from 4.08 ± 0.25 km^2 to 3.78 ± 0.06 km^2 (- 7.4%) and its volume change was – 83.00 ± 3.11 mil m^3 (- 28.6%) between 1990 and 2013. The largest length and areal loss was observed in the smallest niche glacier EB. FB retreated by 263.2 ± 19.0 m and lost 0.26 ± 0.10 km^2

(- 31.4%) of its area between 1990 and 2014. EB retreated by 834.9 ± 7.1 m and lost 0.34 ± 0.07 km^2 (- 75.1%) of its area between 1990 and 2015. The volume of smaller glaciers FB and EB decreased by 6.29 ± 0.71 mil m^3 (- 48.1%) and 5.38 ± 0.50 mil m^3 (- 74.2%), respectively. Our glaciological survey suggests that all the investigated glaciers were subjected to a similar retreat and thinning as other land-terminating glaciers in the different regions of Svalbard (Kohler et al., 2007; Laparazan et al., 2013; Navarro et al., 2014). The intensive glacier recession and ice loss was found to be caused by increase in the mean summer temperature, which occurred at an average rate of 0.51 °C per decade over the period 1992–2012 (Norwegian Meteorological Institute, 2019b).

The maximum ice thicknesses measured by GPR are 135.2 ± 4.8 m at BB, 42.1 ± 1.5 m at FB and 50.5 ± 1.8 m at EB. Mean ice thickness range from 13.3 ± 0.5 (FB), 21.2 ± 0.8 (EB) to 52.5 ± 1.9 (BB). The mean surface lowering of BB was - 23.0 ± 8.4 m between 1990 and 2013, whereas the smaller glaciers FB and EB experienced an average decrease of surface elevation of 22.3 ± 10.2 m between 1990 and 2015 and 10.7 ± 7.8 m between 1990 and 2014 respectively. The thinning was observed almost on the whole surface of glaciers except for the upper parts of EB. The glacier mean thinning over the investigated period was 1.0 ± 0.4 $m.a^{-1}$ (BB), 0.9 ± 0.4 $m.a^{-1}$ (FB) and 0.4 ± 0.3 $m.a^{-1}$ (EB). These high rates of thinning will lead to a considerable or complete melt-out of all the investigated glaciers during 21th century.

Acknowledgements

The research was financially supported by the Charles University Grant Agency, project number 238216. The author sincerely appreciates the opportunity to use the Czech Arctic Research Infrastructure 'Josef Svoboda Station' in Svalbard. The Centre for Polar Ecology of the University of South Bohemia in České Budějovice is thanked for this. We are grateful to Jan Kavan for logistical support during the field research and Zdeněk Stachoň, Tomáš Uxa, Martin Hložek and Tereza Krchňavá for the field assistance. We would like to thank the Norwegian Polar Institute for providing the aerial photographs (1990 and 2009) and the ESA for Sentinel-2 image. The authors also kindly thank the editor and reviewers for their constructive comments.

Appendix A. Supplementary data

Supplementary data to this article can be found online at https://doi.org/10.1016/j.polar.2019.05.004.

References

Ai, S., Wang, Z., D, E., Holmén, K., Tan, Z., Zhou, Ch, Sun, W., 2014. Topography, ice thickness and ice volume of the glacier Pedersenbreen in Svalbard, using GPR and GPS. Polar Res. 33. https://doi.org/10.3402/polar.v33.18533.

Baelum, K., Benn, D.,I., 2011. Thermal structure and drainage system of a small valley glacier (Tellbreen, Svalbard), investigated by ground penetrating radar. Cryosphere 5 (1), 139–149.

Bach, E., Radic, V., Schoof, C., 2018. How sensitive are mountain glaciers to climate change? Insights from a block model. J. Glaciol. 64 (244), 247–258. https://doi.org/10.1017/jog.2018.15.

Førland, E.J., Benestad, R., Hanssen-Bauer, I., Haugen, J.E., Skaugen, T.E., 2011. Temperature and precipitation development at Svalbard 1990 – 2100. Adv. Meteorol. 14. https://doi.org/10.1155/2011/893790.

Hagen, J.O., Melvold, K., Pinglot, F., Dowdeswell, J.A., 2003. On the net mass balance of the Glaciers and Ice caps in Svalbard, Norwegian Arctic. Arctic Antarct. Alpice Res. 35, 264–270.

Hall, D.K., Bayr, K.J., Schöner, W., Bindschadler, R.A., Chien, J.Y.L., 2003. Consideration of the errors inherent in mapping historical glacier positions in Austria from the ground and space (1893 – 2001). Rem. Sens. Environ. 56, 566–577.

Houlding, S.W., 2000. Practical Geostatistics: Modelling and Spatial Analysis. Springer, Berlin, Heidleberg.

IPCC, 2007. In: Solomon, S., Quin, D. (Eds.), Climate Change 2007: the Physical Science Basis. Contribution of Working Group I to the Fourth Assesment Report of the Intergovernmental Panel on Climate Change. Cambridge University Press.

IPCC, 2013. Climate Change 2013, the Physical Science Basis, Working Group I Contribution to the Fifth Assessment Report of the Intergovernmental Panel on Climate Change. WMO/UNEP. Cambridge University Press, Geneva.

James, T.D., Murray, T., Barrand, N.E., Sykes, H.J., Fox, A.J., King, M.A., 2012. Observations of enhanced thinning in the upper reaches of Svalbard glaciers. Cryosphere 6, 1369–1381.

Kohler, J., James, T.D., Murray, T., Nuth, C., Brandt, O., Barrand, N.E., Aas, H.F., 2007. Acceleration in thinning rate on western Svalbard glaciers. Geophys. Res. Lett. 34. https://doi.org/10.1029/2007GL030681.

König, M., Nuth, C., Kohler, J., Moholdt, G., Peterssen, R., 2014. A digital glacier database for Svalbard. In: Kargel, J.S., Leonard, G.J., Bishop, M.P., Kääb, A., Raup, B.H. (Eds.), Global Land Ice Measurements from Space. Springer, Heidelberg, pp. 229–239. https://doi.org/10.1007/978-3-540-79818-7_10.

Laparazan, J., Petlicki, M., Navarro, F., Machio, F., puczko, D., Glowacki, P., Nawrot, A., 2013. Ice volume changes (1936-1990-2007) and ground-penetrating radar studies of Ariebreen, Hornsund, Spitsbergen. Polar Res. 32, 1–10.

Lapazaran, J., Otero, J., Martín-Español, A., Navarro, F., 2016. On the errors involved in ice-thickness estimates I: ground-penetrating radar measurement errors. J. Glaciol. 62 (236), 1008–1020. https://doi.org/10.1017/jog.2016.93.

MALÅ Geoscience, 2005. Ramac GPR. Hardware Manual. MALÅ Geoscinece, Malå.

Malecki, J., 2013a. Elevation and volume changes of seven Dickson Land glaciers, Svalbard, 1630-1990-2009. Polar Res. 32. https://doi.org/10.3402/polar.v32i0.18400.

Malecki, J., 2013b. The Present-Day State of Svenbreen (Svalbard) and Changes of its Physical Properties after the Termination of the Little Ice Age. PhD thesis. Adam Mickiewicz University, Poznań, Poland.

Malecki, J., 2016. Accelerating retreat and high-elevation thinning of glaciers in central Spitsbergen. Cryosphere 10, 1317–1329.

Martin-Español, A., Navarro, F.J., Otero, J., Laparazan, J.J., Blaszczyk, M., 2015. Estimate of total volume of Svalbard glaciers, and their potential contribution to sea-level rise, using new regionally based scaling relationships. J. Glaciol. 61, 29–41.

Martín-Moreno, R., Álvares, F.A., Ove Hagen, J., 2017. Little Ice Age glacier extension and retreat in Svalbard archipelago. Holocene 27 (9), 1379–1390.

Moholdt, G., Nuth, C., Hagen, J.O., Kohler, J., 2010. Recent elevation changes of Svalbard glaciers derived from ICESat laser altimetry. Remote Sens. Environ. 114, 2576–2767.

Navarro, F.J., Martín Espanol, A., Laparazan, J.J., Grabiec, M., Otero, J., Vasilenko, E.V., Puczko, D., 2014. Ice volume estimates from ground-penetrating radar surveys, Wedel Jarlsberg land glaciers, Svalbard. Arctic Antarct. Alpine Res. 46, 394–406.

Nuth, C., Moholdt, G., Kohler, J., Hagen, J.O.,, Kaab, A., 2010. Svalbard glacier elevation changes and contribution to sea liver rise. J. Geophys. Res. 115, 1–16.

NPI, 1990. Aerial Photograph S90_1966. Tromsø. Norwegian Polar Institute.

NPI, 2009. Aerial Photograph S2009_13822_00031_rep and S2009_13822_00033_rep. Tromsø. Norwegian Polar Institute.

Norwegian Polar Institute, 2014. Terrengmodell Svalbard (S0 Terrengmodell). Tromso, Norway. Norwegian Polar Institute. http://data.npolar.no/dataset/dce53a47-c726-4845-85c3-a65b46fe2fea, Accessed date: 5 December 2017.

Norwegian Meteorological Institute, 2019a. Air Temperature in Svalbard, Annual Mean. Environmental monitoring of Svalbard and Jan Mayen (MOSJ) URL: http://www.mosj.no/en/climate/atmosphere/temperature-precipitation.html.

Norwegian Meteorological Institute, 2019b. Seasonal Temperatures for Svalbard Airport. Environmental monitoring of Svalbard and Jan Mayen (MOSJ) URL: http://www.mosj.no/en/climate/atmosphere/temperature-precipitation.html.

Norwegian Meteorological Institute, 2019c. Precipitation in Svalbard and Jan Mayen, Annual Total. Environmental monitoring of Svalbard and Jan Mayen (MOSJ) URL: http://www.mosj.no/en/climate/atmosphere/temperature-precipitation.html.

Palli, A., Moore, J.C., Jania, J., Glowacki, P., 2003. Glacier changes in southern Spitsbergen, Svalbard, 1901-2000. Ann. Glaciol. 37, 219–225.

Radić, V., Bliss, A., Beedlow, A.C., Hock, R., Miles, E., Cogley, J.G., 2014. Regional and global projections of twenty-first century glacier mass changes in response to climate scenarios from global climate models. Clim. Dyn. 42 (1–2), 37–58. https://doi.org/10.1007/s00382-013-1719-7.

Rachlewicz, G., Szczuciński, W., Ewertowstki, M., 2007. Post-"Little Ice Age" retreat rates of glaciers around -billefjorden in central Spitsbergen, Svalbard. Pol. Polar Res. 28 (3), 159–186.

Rivera, A., Benham, T., Casassa, G., Bamber, J., Dowdeswell, J.A., 2007. Ice elevation and areal changes of glaciers from the northern Patagonia icefield, Chile, global planet. Change 59 (1 – 4), 126–137. https://doi.org/10.1016/j.gloplacha.2006.11.037.

Sandmeier, K.J., 2008. REFLEXW: Processing Program for Seismic, Acoustic and Electromagnetic Reflection, Refraction and Transmission Data. Sandmeier Scientific Software, Karlsruhe Version 5.0.

Serreze, M.C., Francis, J.A., 2006. The Arctic amplification debate. Clim. Change 76, 241–264. https://doi.org/10.1007/s10584-005-9017-y.

Slangen, A.B.A., Carson, M., Katsman, C.A., van de Wal, R.S.W., Köhl, A., Vermeersen, L.L.A., Stammer, D., 2014. Projecting twenty-first century regional sea-level changes. Clim. Change 124 (1–2), 317–332. https://doi.org/10.1007/s10584-014-1080-9.

Snow, Water, Ice and Permafrost in th Arctic (SWIPA), 2017. Arctic Monitoring and Assessment Programme (AMAP). Oslo.

TRIMBLE, 2008. GPS Pathfinder Office Software Getting Started Guide. pp. 176.

TRIMBLE, 2009. GeoExplorer 2008 Series User Guide. Westminster, Trimble Navigation Ltd.

Zheng, W., Pritchard, M.E., Willis, M.J., Tepes, P., Gourmelen, N., Benham, T.J., Dowdeswell, J.A., 2018. Accelerating glacier mass loss on Franz Josef land, Russian Arctic. Remote Sens. Environ. 211, 357–375.